EPJ Web of Conferences **86**, 00046 (2015)
DOI: 10.1051/epjconf/ 20158600046

Incomplete fusion reactions in ^{16}O+^{159}Tb system: Spin distribution measurements

Vijay R. Sharma[1,a], Abhishek Yadav[2], Devendra P. Singh[3], Pushpendra P. Singh[4], Sunita Gupta[5], Manoj K. Sharma[6], Indu Bala[2], R. Kumar[2], S. Muralithar[2], R. P. Singh[2], B. P. Singh[1,b], R. Prasad[1], and R. K. Bhowmik[2]

[1] *Department of Physics, Aligarh Muslim University, Aligarh 202 002, India*
[2] *NP-Group, Inter University Accelerator Centre, New Delhi - 110 067, India*
[3] *Department of Physics, CoE, University of Petroleum & Energy Studies, Dehradun - 248 007, India*
[4] *Department of Physics, Indian Institute of Technology Ropar, Punjab 140 001, India,*
[5] *Physics Department, Agra College, Agra- 282 001, India*
[6] *Physics Department, S. V. College, Aligarh - 202 001, India*

Abstract. In order to explore the reaction modes on the basis of their entry state spin population, an experiment has been done by employing particle-γ coincidence technique carried out at the Inter University Accelerator Centre, New Delhi. The preliminary analysis conclusively demonstrates, spin distribution for some reaction products populated via complete and/or incomplete fusion of ^{16}O with ^{159}Tb system found to be distinctly different. Further, the existence of incomplete fusion at low bombarding energies indicates the possibility to populate high spin states.

1 Introduction

The study of incomplete fusion (ICF) of heavy ions with different projectile-targets combination has been a topic of renewed interest at energies near and above the Coulomb barrier [1, 2]. Observations show that at the presently studied energies ($\approx$ 4-7MeV/A), the dominant nuclear reaction mechanisms are complete fusion (CF) and the ICF [3–6]. Efforts are still in progress to gain better understanding of ICF processes. Britt and Quinton [7] were the first to observe the production of forward-peaked fast α particles in the breakup of the ^{12}C, ^{14}N and ^{16}O projectiles at energy $\approx$ 10.5 MeV/A. Advances in the understanding of ICF dynamics were made after the charged particle-γ coincidence measurements by Inamura et al. [8]. On the basis of semi-classical theory of heavy ion (HI) reactions, the CF and ICF processes are broadly categorized on the basis of driving input angular momentum ℓ imparted into the system. In the CF process the driving input angular momentum $0 \leq \ell \leq \ell_{crit}$, in accordance with a sharp cutoff approximation and may be understood in the following way. In case of CF, the attractive nuclear potential overcomes the repulsive Coulomb and centrifugal potentials in central and near-central collisions. Hence, CF process takes place at a small values of impact parameter at which the formation of fully equilibrated compound nucleus (CN) takes place. On the other hand, at relatively higher values of impact parameter, a competition between repulsive centrifugal and attractive nuclear potential results in the breakup of the projectile. Therefore, an incompletely fused composite system comprising of a part of the projectile and the target appears in the exit channel that leads to the ICF process, wherein the involvement of driving input angular momentum ℓ is relatively larger than that needed for the CF process to take place. Quantitatively, the driving input angular momentum exceeds the critical limit (ℓ_{crit}) for CF and hence, no fusion can occur unless a part of the projectile is emitted to release the excess driving input angular momentum. As such, prompt emission of a part of the projectile (predominantly α clusters) takes place to provide sustainable input angular momenta to the system (e.g., ^{16}O breaks into ^{12}C and α particle). After such an emission, the resulting angular momenta carried by the remnant projectile is less than or equal to its own critical angular momentum limit for fusion to occur with the target nucleus. Hence, in case of ICF the residual nuclei produced is therefore assumed to be associated with ℓ values above ℓ_{crit} for CF. It may be relevant to mention here that, Tserruya et al. [9] showed that ICF processes may contribute significantly below and above input angular momentum limits and there is no sharp cutoff limit of input angular momentum.

Further, the ICF reaction studies by charged particle-γ coincidence technique have been carried out with low-Z (Z $\leq$ 10) projectile-induced reactions on heavy targets (A $>$ 150). However, such information is scarce for medium mass target nuclei. Several models [4] have been used to fit the experimental data obtained at energies well above the Coulomb barrier (i.e., $E_{lab} \geq$ 10.5 MeV/A) but have shown certain failings in their ability to explain ICF data at relatively low bombarding energies (i.e.,$\approx$ 3-7 MeV/A.

[a] e-mail: phy.vijayraj@gmail.com
[b] e-mail: bpsinghamu@gmail.com

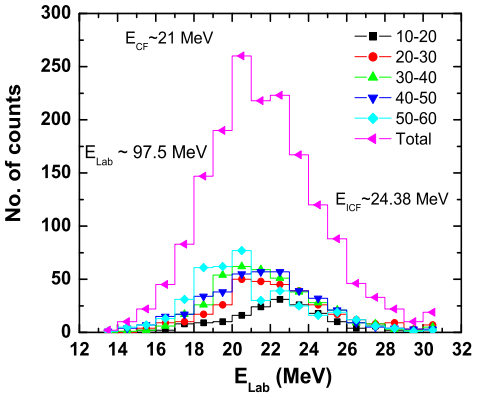

Figure 1. (Color online) Fusion-evaporation (CF) α-energy profile for forward (F) zone (10^0-60^0) at projectile energy E = 97.5 ± 1.5 MeV in the ^{16}O + ^{159}Tb system predicated by PACE4. Different angular slices from 10^0 to 60^0 are also shown in this figure.

Hence, the study of ICF dynamics is still an active area of investigation.

Recent studies on spin distributions for the system ^{16}O + ^{169}Tm at ≈ 90 MeV beam energy show significantly different patterns in the spin distributions for the reaction products produced by CF and ICF processes [10, 11]. To get more information about input angular momentum involved for various degrees of ICF dynamics, a particle-γ coincidence experiment has been performed for the system ^{16}O + ^{159}Tb at ≈ 4-7MeV/A projectile energy. In this paper, spin distributions for various evaporation residues (ERs) have been identified and are reported. This paper explains our preliminary results of spin distribution measurements for CF and ICF residues in ^{16}O+^{159}Tb system at ≈ 97.5 ± 1.5 MeV beam energy.

2 Experimental Setup and Data Reduction Methodology

Aiming to investigate the high ℓ values in successively opened ICF channels and to test the possibility of populating high-spin states in final reaction products via ICF, a particle-γ coincidence experiment was performed at the Inter-University Accelerator Center (IUAC), New Delhi, India. In the present work, spin distributions of CF and ICF products has been measured at 99 MeV beam energy. An isotopically pure Terbium (^{159}Tb, abundance ≈ 100%) target of thickness 1.79 mg/cm^2 was bombarded by ^{16}O^{6+} with beam current ≈ 30-35 nA. Target thickness was measured by an α-transmission method. This technique is based on the measurement of the energy loss per unit path length by ≈ 5.487 MeV α particles obtained from a standard ^{241}Am source, while passing through the target material. In the present section brief details of experimental setup and data reduction methodology are discussed.

2.1 Experimental Setup

In the present work, coincidences are recorded using the γ-detector array (GDA) along with an array of charged particle detectors (CPDs) to identify the different reaction channels. The GDA consists of 12 Compton-suppressed high resolution high-purity germanium (HPGe) γ spectrometers arranged at three angles with respect to the beam axis, i.e., 45^0, 99^0, and 153^0, and four detectors installed at each of these angles. The array of CPDs is an assembly of 14-phoswich detectors arranged in two truncated hexagonal pyramids, the bases of these pyramids lie in a horizontal plane with each having a trapezoidal shape. The top and bottom spaces are filled by two hexagonal detectors that, together with trapezoids, cover ≈ 90% of the total solid angle. In order to employ different gating conditions and to detect particles (Z = 1, 2) in coincidence with prompt γ rays at various angles, the array of CPDs was divided into three angular zones (i) forward (F) 10^0-60^0, (ii) sideways (S) 60^0-120^0, and (iii) backward (B) 120^0-170^0. The coincidences were demanded between particles (Z = 1, 2) and prompt-γ rays by employing three gating conditions corresponding to the given angular zones for each value of Z. Depending on the fast and slow components of the CPDs, particles (a sum of protons and α's) and α's in each angular zone were detected in coincidence with prompt-γ rays. As a matter of fact, the CPDs at forward (F) angles (10^0-60^0) are expected to detect both slow and fast α components; i.e., (i) slow α component: fusion-evaporation (CF) α particles, and (ii) fast α component: direct α particles associated with ICF. The energy profile of slow α particles (emitted from fully equilibrated CN) was generated by the theoretical model code PACE4 [12] (see Fig. 1). This code is based on the statistical approach of CN de-excitation by Monte Carlo procedure and was extensively used for CN-related calculations in past years. Similar input parameters, as in Ref. [11], are used for this calculation. As can be seen in Fig. 1, the theoretically estimated most probable energy of slow α particles (E_α^{CF}) is found to be ≈ 21 MeV at 97.5 ± 1.5 MeV beam energy. However, the energy of the fast α component (E_α^{ICF}) can be calculated as projectile energy times ejectile-projectile mass ratio, and comes out to be ≈ 24.37 MeV at 97.5 ± 1.5 MeV for the ^{16}O beam. As such, the gating condition i.e. backward α-gated spectra is subtracted from the forward α-gated spectra were used, so that only fast α component in the forward cone can be detected.Further, an Al absorbers of appropriate thickness (estimated by the SRIM08 code [13] based on the range-energy formulation) were used to stop the elastic scattering from ^{16}O beam. Multiparameter, particle-γ-coincidence data are recorded in the list mode, which includes different gating conditions such as particle(s)/α detected in backward (B), forward (F), and sideways (S) angles. Singles data were collected to identify xn channels predominantly populated via CF.

2.2 Data Analysis

Off-line data analysis was performed in steps using the nuclear physics data analysis software INGAsort [14]. In the

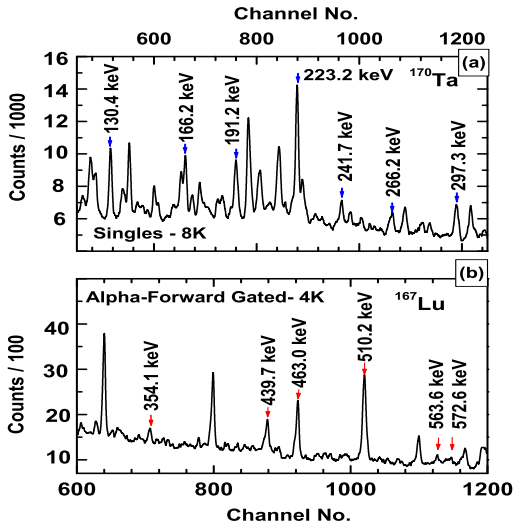

Figure 2. (Color online) Typical γ-spectrum for the ^{16}O + ^{159}Tb interaction at 97.5 ± 1.5 MeV, where γ-lines are assigned to the bands identified for the CF and/or IF residues. (a) Singles (b) forwarded alpha-gated spectra.

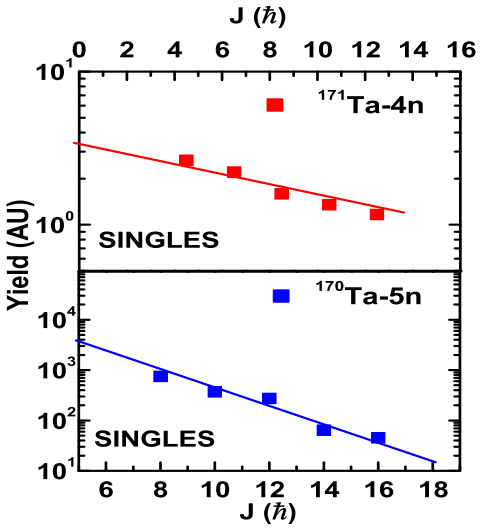

Figure 3. (Color online) Experimentally measured spin distributions for CF-4n, 5n channel (identified from singles spectra). Reaction products are labeled by self-explanatory notations and emission cascades. Lines through the data points are drawn to guide the eyes.

first step, the energy calibration and gain matching of the HPGe detectors were carried out by counting standard radioactive γ source (^{152}Eu) before and after the experiment precisely at the target position. In the second step, particle-γ-coincidence spectra were generated to identify different reaction channels. Various gating conditions are projected onto the γ spectra to generate particle-gated spectra for each angular zone. Assuming isotropic γ emission, all gated spectra for a particular gating condition are summed up to improve the event statistics. The different reaction products populated via CF and/or ICF are identified on the basis of their characteristic γ lines by looking into the particle gated and/or singles spectra. The xn channel are identified from singles spectra recorded by two coaxial HPGe detectors. In order to identify pxn channels populated via CF, backward (B)-α gated spectra are subtracted from backward (B) particle-gated spectra to generate pure backward (B)-proton-gated spectra. The CF αxn channels (consisting of slow α component) are identified from the backward (B)-α-gated spectra. Further, as expected in ICF, the direct α particles (associated with ICF) are supposed to be concentrated only in the forward (F) cone. It may further be pointed out that the slow α component (associated with CF) coming from the de-excitation of CN may also be emitted in the forward cone due to the isotropic nature of the particle emission in CN reactions. As was already mentioned in the previous section, the slow α component is filtered out by putting an Al absorber on forward cone CPDs. However, to remove any contamination from the slow α component in the forward (F) cone, backward (B)-α-gated spectra are subtracted from the forward (F)-α-gated spectra. The ICF channels are identified from forward (F)-α-gated spectra (corrected for slow α-component). The relative production yield of the identified reaction products are deduced from the intensity of the photopeak of characteristic prompt γ transitions assigned to a particular reaction product. Spectroscopic data, such as prompt γ energies and their intensities, are taken from the NNDC and RADWARE level scheme directory [15, 16]. Further, it may be pointed out that the relative number of statistical and "yrast"-like transitions depend on the entry state angular momenta and the available excitation energy (E*). The CF reaction products are formed at high E* and low angular momenta leading to more statistical transitions, where "yrast" states are expected to be fed by statistical γ transitions. However, the ICF reaction products may achieve low E* (due to the involvement of partial degrees of excitations) and high angular momenta (relatively higher values of impact parameters contribute to the high-spin states) at a given projectile energy. In such a case, the number of "yrast"-like transitions are expected to be much larger than that of the statistical ones, where less or no feeding is expected. Therefore, the spin distributions of CF and ICF products are expected to be entirely different in nature and can be used as a sensitive tool to probe reaction dynamics by looking into the entry state spin population [17]. As such, to have an insight into the decay patterns of CF and ICF reaction products, spin distributions of different reaction products were generated.

3 Results and Discussion

As has already been discussed that events were collected with particle-γ coincidences given by the HPGe Compton suppressed detectors and Phoswich detectors. The CF channels ^{171,170}Ta were identified from the background suppressed singles spectra. In order to increase the statistics, the gain matched γ-ray spectra of HPGe detectors

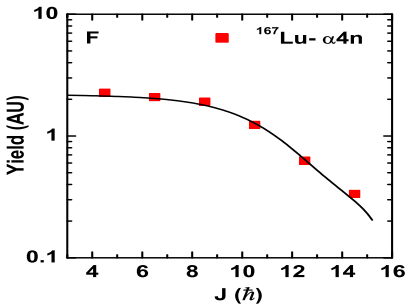

Figure 4. (Color online) Experimentally measured spin distributions for ICF-α4n channel (identified from forward α-gated spectra). Reaction products are labeled by self-explanatory notations and emission cascades. Lines through the data points are drawn to guide the eyes.

were summed up. As a representative case, Fig. 2(a and b) shows the typical singles and forwarded alpha-gated spectra. The selection of the rotational band for ^{170}Ta residues has been obtained from the level scheme [18] and the peaks are assigned for the characteristics γ-lines in Fig. 2(a). Relative production yields as a function of experimentally observed spin (J) for ^{170}Ta alongwith ^{171}Ta populated via CF only are plotted in Fig 3. The errors have not been shown in the figures as they have been estimated to be $\leq 10\%$ and the inclusion of these errors is not likely to modify the present analysis. The measured spin distribution profile for ICF residues ^{167}Lu (α4n channel) is plotted in the Fig.4, where, the selection of the band for this channel has been obtained from the level scheme [19]. It may be mentioned that Figs. 3 and 4 show the experimentally measured relative production yield as a function of spins (J) which is termed as 'spin distribution' [11].

The nomenclature 'F' used in Fig.4 indicates the involved reaction dynamics for ICF-channel i.e., identified from forward(F)-α-gated spectra. As can be observed from the figures 3 and 4, in general, there is a strikingly different behavior of the spin-distribution patterns for different channels which indicates the involvement of entirely different reaction dynamics in the production of these reaction products. The intensity of xn(singles) (populated via CF only) falls off rather quickly with observed spin (J), indicating strong feeding and/or broad spin population during the de-excitation of CN. However, for αxn-F-channels (expected to be populated via ICF), the intensity appears to be almost constant up to a certain value of J, and then decreases towards high angular momentum. This indicates the absence of feeding to the lowest members of the 'yrast' band and/or the members of the 'yrast' band and/or the population of low spin states are strongly hindered in the ICF channels.

4 Summary

This paper gives the recent preliminary experimental results for the particle-γ coincidence experiment. The identified xn (populated via CF) and αxn (populated via ICF) channels indicate the different de-excitation patterns on the basis of entry state spin. In order to understand the magnitude of mean driving angular momenta (ℓ-values), and to examine the possibility to populate high spin states via ICF, mean driving angular momenta involved in CF and ICF channels will be deduced from the analysis of spin-distributions.

Acknowledgements

The authors thank to the Chairman, D/o Physics, AMU, Aligarh & the Director, IUAC, New Delhi, for providing all the necessary facilities to carry out this work. RP, BPS, DPS and VRS thanks to the DST: SR/S2/HEP-30/2012 for providing financial support.

References

[1] P. R. S. Gomes *et al.*, Phys. Lett. B **601**, 20 (2004).
[2] M. Dasgupta *et al.*, Nucl. Phys. A **787**, 144 (2007).
[3] A. Yadav *et al.*, Phys. Rev. C **86**, 014603 (2012); ibid **85**, 034614 (2012); ibid **85**, 064617 (2012) and references therein.
[4] Vijay R. Sharma *et al.*, Phys. Rev. C **89**, 024608 (2014), ibid., **84**, 014612 (2011).
[5] Devendra P. Singh *et al.*, Phys. Rev. C **89**, 024612 (2014).
[6] M. Cavinato *et al.*, Phys. Rev. C **52**, 2577 (1995).
[7] H. C. Britt and A. R. Quinton, Phys. Rev. **124**, 877 (1961).
[8] T. Inamura *et al.*, Phys. Lett. B **68**, 51 (1977).
[9] I. Tserruya *et al.*, Phys. Rev. Lett. **60**, 14 (1988).
[10] P. P. Singh *et al.*, Phys. Rev. C **78**, 017602 (2008).
[11] P. P. Singh *et al.*, Phys. Lett. B **671**, 20 (2009).
[12] O. B. Tarasov and D. Bazin, Nucl. Instrum. Methods Phys. Res., Sect. B **204**, 174 (2003).
[13] SRIM06; [http://www.srim.org/].
[14] R. K. Bhowmik, S. Muralithar, and R. P. Singh, DAE-Nucl. Phys. Symp. **44B**, 422 (2001); **44B**, 382 (2001) (private communication).
[15] http://www.nndc.bnl.gov/
[16] RADWARE, the level scheme directory on http://radware. phy.ornl.gov/agsdir1.html.
[17] G. J. Lane, G. D. Dracoulis, A. P. Byrne, A. R. Poletti, and T.R. McGoram, Phys. Rev. C **60**, 067301 (1999), and references therein.
[18] Y. H. Zhang *et al.*, Phys. Rev. C **60**, 044311 (1999).
[19] C. H. Yu *et al.*, Nucl. Phys. A **511**, 157 (1990).